

# Seasonal Variations in Diurnal Temperature Range From Satellites and Surface Observations

Donglian Sun, Menas Kafatos, Rachel T. Pinker, and David R. Easterling

**Abstract**—The diurnal temperature range (DTR) is an important climate-change variable and, until recently, it was derived from station observations of surface air temperature ( $T_a$ ). Station-based observations are sparse and unevenly distributed, making the use of satellites an attractive option for evaluating DTR. In this study, satellite-based estimates of DTR are evaluated against ground measurements of surface skin temperature ( $T_s$ ) and compared with weather-station observations based on  $T_a$ . Geographical and seasonal differences were identified in both ground- and satellite-derived DTRs. Estimates of DTR from station-observed air temperature represent all-sky conditions while satellite estimates of DTR from surface skin temperature represent clear conditions only. For both station observations and satellite estimates, DTRs at rural locations tend to be larger than at urban sites. The DTRs based on  $T_s$  are larger than those derived from  $T_a$  under both all and clear-sky conditions. Clouds tend to reduce the magnitude of the DTR. The station-observed DTRs are found to be larger in summer than in winter over the entire U.S. The satellite-derived DTRs are larger in spring and fall than in winter and summer over the eastern U.S., while they are larger in spring and summer than in fall and winter over the western part. Evapotranspiration from land vegetation and the effects of water-vapor radiative forcing have a major effect on the detected spatial and seasonal variations in the DTR patterns.

**Index Terms**—Diurnal temperature range (DTR), effects of evapotranspiration, satellite-derived DTR, station observations of DTR, water-vapor radiative forcing (WRF) on DTR.

## I. INTRODUCTION

THE DIURNAL temperature range (DTR) is an important index of climate change [1] because DTR is susceptible to a variety of environmental effects including water vapor, cloudiness, and urban influences [2]. Until recently, most information on this parameter came from station air temperature ( $T_a$ ) observations. During recent decades, DTR has been observed to decrease over the U.S. [3], [4] as well as over the globe [1], [5]. Kalnay and Cai [4] explain that this may be due to the impact of land-use changes, such as urbanization and agricultural development, while Trenberth [6] and Stone and Weaver [7] point out that changes in clouds and surface

Manuscript received September 14, 2005; revised January 4, 2006. This work was supported by the NASA Science Applications Program under the VAccess/MAGIC project of George Mason University. The work that resulted in the DTRs was supported by the NOAA Office of Global Programs under Grant NA030AR4310045 and Grant NA06GP0404, which were awarded to the University of Maryland.

D. Sun and M. Kafatos are with George Mason University, Fairfax, VA 22030 USA.

R. T. Pinker is with the University of Maryland, College Park, MD 20742 USA.

D. R. Easterling is with the National Climatic Data Center, Asheville, NC 28801 USA.

Digital Object Identifier 10.1109/TGRS.2006.871895

moisture have also an impact on the observed trends in DTR. Several recent studies based on climate model simulations suggest that DTR changes may be due to the effects of human-induced increase in atmospheric greenhouse gases ( $\text{CO}_2$ ) and sulfate aerosols [8]–[10]; however, Zhao and Pitman [11] point out that the increase in greenhouse gases affects both the maximum and minimum temperature and, consequently, their influence on the changes in DTR is small.

Gallo *et al.* [12] evaluated the diurnal range of  $T_a$  over the U.S. using the data from the U.S. Historical Climatology Network (USHCN). They found that rural stations tended to have larger diurnal range than urban stations, and that the diurnal range of  $T_a$  during the summer months was larger than during the winter months. Surface skin temperature  $T_s$  (radiative temperature) is directly relevant to surface–atmosphere energy exchange, and tends to have a stronger urban heat island (UHI) signal than  $T_a$  [13]. The satellite-derived DTR from  $T_s$  is different in nature than station-observed DTR of  $T_a$ , since satellites observe  $T_s$  under clear-sky conditions only, while station-observed  $T_a$  integrates the effects of clouds. Therefore, the station-observed DTR from  $T_a$  includes the feedback effect of clouds on climate change, which may be more difficult to interpret, because uncertainties exist about cloud-cover extent. Dai *et al.* [14] point out that clouds have increased during the last 4–5 decades over the U.S. and many other regions where DTR was reported to decrease. More recent studies based on global-scale satellite observations claim that there has been a steady decrease in cloudiness in the last 20 years [15].

Satellite observations allow for homogeneous spatial sampling and therefore, it is of interest to evaluate satellite based estimates of DTR. Most satellite estimates of  $T_s$  are based on observations from polar orbiters due to their spatial resolution and global coverage. Surface temperature, especially land surface temperature (LST), has a strong diurnal cycle, which cannot be captured at the temporal resolution (approximately two times per day) of the polar orbiters. Jin and Dickinson [16] estimated the diurnal range of surface skin temperature from the twice-daily observations of the polar imager Advanced Very High Resolution Radiometer (AVHRR) using a diurnal-cycle pattern based on climate model simulations. Jin *et al.* [13] also calculated a difference in skin temperature from the monthly mean daytime minus monthly mean nighttime skin temperature from Moderate Resolution Imaging Spectroradiometer (MODIS) observations. However, these do not represent a real diurnal range of skin temperature. Geostationary satellites provide high temporal coverage, which makes them attractive for deriving information on the diurnal cycle

of LST. Sun and Pinker [17], [18] introduced a new split window algorithm for LST retrieval from the Geostationary Operational Environmental Satellite (GOES-8) and showed that accuracy better than 1 K can be obtained for the retrieved LST. Although the spatial resolution for a geostationary satellite (4 km at nadir for GOES) may be lower than for polar orbiters (1 km at nadir for AVHRR or MODIS infrared), the LST retrievals from GOES are of similar quality to those of MODIS LST ( $\pm 1$  K accuracy) [19].

To be of use as a climate index, the systematic error in the measurement must be less than the magnitude of scientifically relevant climatic change. Suppose that the sensors used to measure surface air temperature in the century preceding 1950 had an accuracy of  $\pm 1$  °C. Such a record would still be useful in climate studies, and it would be possible to detect long-term trends in the amplitude of the diurnal cycle (DTR) [21]. In order for meteorological observations from space to form the basis of a climate record that will be useful for investigating climate variability, the observations must meet the standards we require of ground-based records. The accuracy of GOES-based  $T_s$  retrievals is better than 1 °C and, therefore, would be useful for detecting climate-change impact on DTR.

In this study, the diurnal range of  $T_s$  is derived from GOES-8 observations using the algorithms described in [17] and [18], and it is compared with corresponding values from ground measurements of  $T_s$  and weather station observations of  $T_a$ . The methodology and data used are briefly described in Section II. Section III discusses the results, and conclusions are provided in Section IV.

## II. DATA AND METHODOLOGY

### A. Data

The National Oceanic and Atmospheric Administration's National Environmental Satellite, Data, and Information Service is generating an operational insolation product from GOES observations, originally, in support of the Global Energy and Water Cycle Experiment (GEWEX) Continental-Scale International Project (GCIP) activities. Information on clear-sky mean brightness temperature, cloud-cover fraction (CCF), and water vapor is available as by-products and archived at the University of Maryland (<http://www.atmos.umd.edu/~srb/gcip>) [20]. These data are used as input to the skin-temperature inference scheme of Sun and Pinker [17], [18] to estimate DTR. Ground observations of upwelling thermal infrared radiation from the Surface Radiation Network (SURFRAD) [22] at two stations (Boulder, CO, and Penn State, PA) and surface skin temperature from the Oklahoma MESONET network are used to evaluate the GOES-8-based DTR.

Monthly mean maximum and minimum surface air temperature for 1221 weather stations is available from the USCHN and can be obtained from NCDS (<ftp://ftp.ncdc.noaa.gov/pub/data/ushcn>) [3], [8], [23] together with independent land use/land cover (LU/LC) information. The USHCN stations are classified according to the following LU/LC nine classes: 0) unknown, 1) nonvegetated or barren, 2) coastal or islands, 3) forest, 4) farmland, savannah, prairie, or tundra, 6) small

TABLE I  
COEFFICIENTS IN (1) FOR LST RETRIEVAL USING  
THE PROPOSED SPLIT WINDOW ALGORITHM [24]

Surface type index	$A_0$	$a_1$	$a_2$	$a_3$	$a_4$
1	-40.8003	1.1379	4.2331	0.6696	440.8983
2	-38.0254	1.1306	2.9363	0.4310	389.1353
3	-22.3312	1.0811	1.2846	0.08122	299.3654
4	-43.5249	1.1429	4.0500	0.8468	372.8079
5	-14.0039	1.0552	3.8472	0.8034	215.8642
6	-19.2040	1.0656	1.6483	0.1664	360.0819
7	-36.4219	1.1247	2.2005	0.2633	405.0694
8	-28.8756	1.0997	0.8253	-0.0443	368.7344
9	-31.9996	1.1101	1.4219	0.1197	319.9049
10	-36.2739	1.1257	2.1882	0.2871	366.3823
11	-24.2080	1.0832	0.0339	-0.2376	334.5423
12	-20.8862	1.0712	1.0017	-0.0233	398.6087
13	118.3286	0.6040	-1.8933	-0.3158	-173.0007

town (< 1000 population), 7) town (1000 to 10 000 population), small city (city with buildings < 10 m tall), 8) large city (city with buildings > 10 m tall), and 9) airport [8]. Based on the above classification, Gallo *et al.* [3] categorized the  $T_a$  data into rural and urban and investigated the seasonal variability in DTR from the station-observed air temperature. To facilitate comparison with the satellite-based DTR, similar categorization will be followed here. Surface soil moisture and evapotranspiration data are obtained from the University of Delaware [24].

### B. LST Retrieval Algorithm

The LST retrieval methodology is described in Sun and Pinker [17]. Briefly

$$T_s(i) = a_0(i) + a_1(i)T_{11} + a_2(i)(T_{11} - T_{12}) + a_3(i)(T_{11} - T_{12})^2 + a_4(i)(\sec \theta - 1) \quad (1)$$

where  $i$  is the index of surface types, and  $\theta$  is the satellite-viewing angle,  $T_{11}$  and  $T_{12}$  are the brightness temperatures at 10.8- and 12.0- $\mu\text{m}$  channels, respectively,  $a_0$  to  $a_4$  are the coefficients, and  $T_s$  is the derived skin temperature. The coefficients in (1) as provided in Table I are derived from the GOES-8 forward simulations using the Moderate Resolution Atmospheric Radiance and Transmittance Model (MODTRAN).

It was found [17] that by using land cover information instead of surface emissivity, the estimates of LSTs from GOES-8

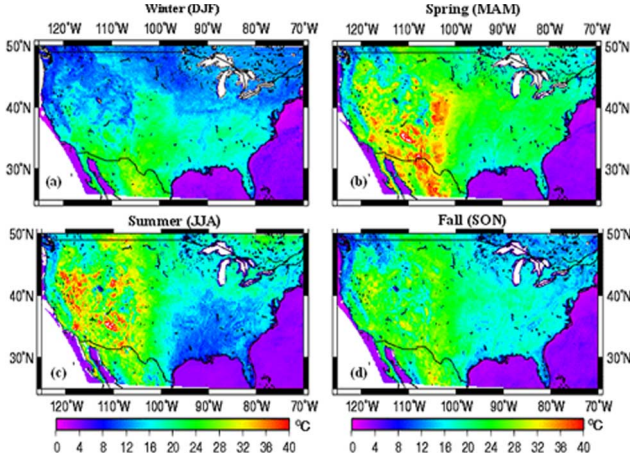


Fig. 1. Spatial distribution of DTR derived from the GOES-8 observations as averaged from 1996 to 2000 during: (a) winter, (b) spring, (c) summer, and (d) fall. The lakes were excluded due to the mixture of water and ice conditions.

measurements using (1) show improvements as compared with previously available split window algorithms that use surface emissivity. The root-mean-square (rms) error for the proposed algorithm is less than 1 K for simulations and 2 K for the actual GOES-8 observations with bias (accuracy) lower (better) than 0.5 K for simulations and  $\pm 1$  K for GOES-8 observations.

The GOES-8 satellite data are available from 1996 to present. The maximum and minimum surface air temperatures from the USHCN weather stations cover the period 1904 to 2000. The period from 1996 to 2000 has been used in this study. Clear conditions (when reported hourly CCF was less than 10%) were selected to calculate  $T_s$ . The retrieved  $T_s$  is used to calculate the DTR (maximum-minimum  $T_s$ ) for clear days (daily CCF < 10%).

### III. RESULTS

#### A. Distribution of Satellite-Based DTR

A five-year (1996–2000) average DTRs for four seasons is illustrated in Fig. 1. Satellite-derived DTRs vary with season and show geographical differences. Larger DTRs are found over the western and central U.S. than over the east and the northwest coast (Fig. 1). It is evident that over the western U.S. (west of  $100^\circ$  W), DTR is larger during warm seasons than in the cold season (winter) (spring has the largest values followed by summer and fall), while over the eastern part (east of  $100^\circ$  W), DTR is larger in spring and fall as compared to winter and summer. Due to the large heat capacity of the oceans, DTR over ocean is usually much smaller than over land.

The geographical differences and seasonal variations in satellite estimates of DTR may be related to the spatial distribution and temporal changes of the surface soil moisture, vegetation cover, evapotranspiration, aerosols, and LC/LU types [25]. A remarkable resemblance between low DTR and high vegetation index is found for all seasons [25]. Evapotranspiration is found to be higher in the east than in the west, especially during summer (Fig. 2). Evapotranspiration from vegetation contributes significantly to the dip of DTR during the warm months in the eastern U.S. [26].

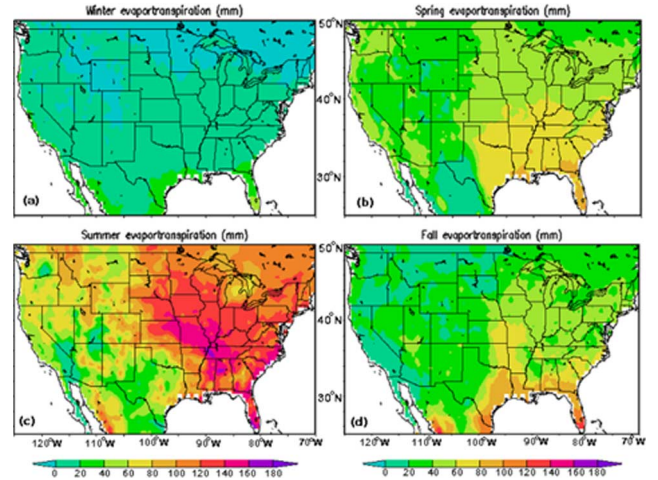


Fig. 2. Spatial distribution of evapotranspiration during (a) winter, (b) spring, (c) summer, and (d) fall.

TABLE II  
EVALUATIONS OF SATELLITE-DERIVED DTRs AGAINST GROUND MEASUREMENTS FOR DIFFERENT MONTHS IN 2000

SURFRAD				
DTR error (K)	Jan. (n=25)	Apr. (n=10)	Jul. (n=30)	Oct. (n=75)
Accuracy	0.5221	-0.2928	0.7613	-0.4993
RMS	1.4747	2.4127	2.9007	1.5654
Precision	1.3791	2.3949	2.7990	1.4836
MESONET				
DTR error (K)	Jan. (n=534)	Apr. (n=534)	Jul. (n=712)	Oct. (n=712)
Accuracy	0.3497	0.7613	-0.6070	0.3161
RMS	1.3021	2.9007	2.7715	0.9986
Precision	1.2542	2.7990	2.7042	0.9472

#### B. Evaluation of DTRs Against Ground Observations

The upwelling thermal irradiance  $R^\uparrow$  measured at the SURFRAD sites in the spectral range of  $3.0\text{--}50.0\ \mu\text{m}$  is converted to surface skin temperature  $T_s$  according to

$$T_s = \left( \frac{R^\uparrow}{\varepsilon\sigma} \right)^{\frac{1}{4}} \quad (2)$$

with surface emissivity  $\varepsilon$  assigned according to surface types, and  $\sigma$  is the Stefan–Boltzmann constant.

Evaluation of the satellite-derived DTR against ground observations shows an accuracy of better than  $\pm 1\ ^\circ\text{C}$ , and an rms error of about  $2\ ^\circ\text{C}$  in spring and summer, and  $1\ ^\circ\text{C}$  in winter and fall (Table II). The error in DTR is found to be of the same magnitude as the error in the  $T_s$  retrieval [17].

#### C. Seasonal Variations in DTR From Satellites and Stations

To compare the variations in the satellite-based DTRs with those derived from station observations, surface skin temperature derived from GOES-8 at hourly intervals is interpolated to the USHCN weather-station locations and then aggregated according to the rural/urban classification of Gallo *et al.* [3]. Specifically, DTR was calculated and averaged for each month for 855 rural stations (classified as forest, farm, small town, and town) and 256 urban stations (small cities, large cities, and airports). A temporal average of DTR for the period from 1996 to 2000 was then calculated for both station observations and satellite estimates, as shown in Fig. 3.

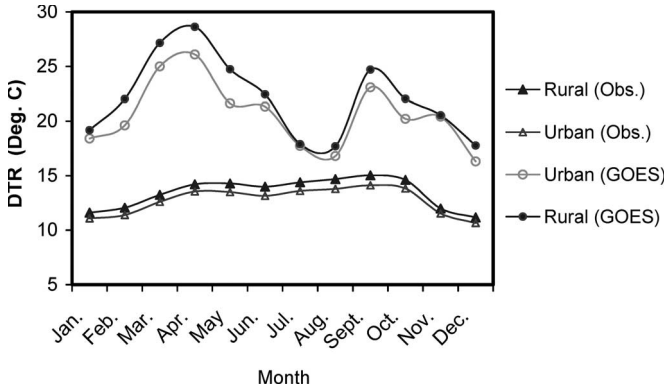


Fig. 3. DTR from station observations under all-sky conditions and satellite retrievals under clear-sky conditions as averaged over rural and urban stations over the U.S. for the period from 1996 to 2000.

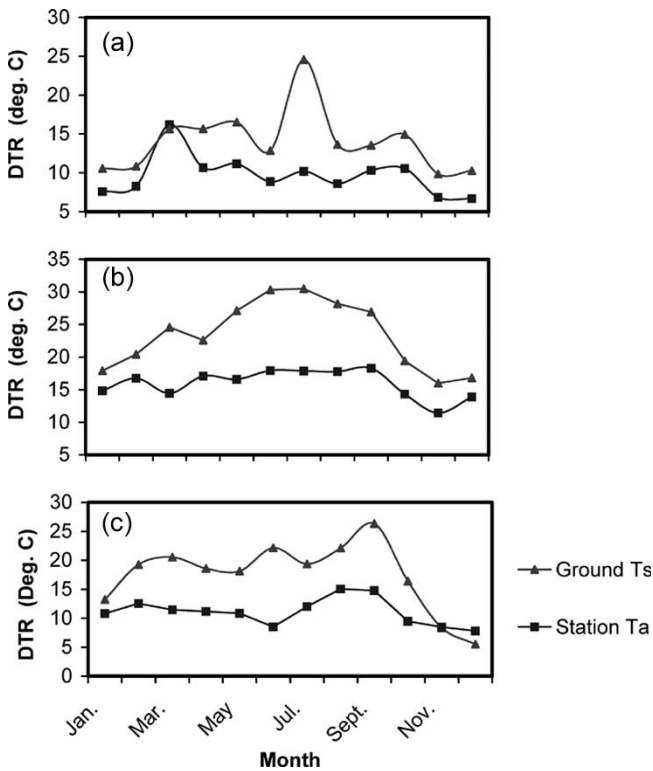


Fig. 4. Comparison of DTR of  $T_a$  from station observations and from ground measurements of  $T_s$  under all-sky conditions at (a) Penn State, PA, (b) Boulder, CO, and (c) Ardmore, OK.

For station observations, the average DTR is found to be larger for rural stations than for urban stations (significant at  $\alpha = 0.05$  or 95% confidence level from the  $t$ -test), in agreement with Gallo *et al.* [12]. Thus, a decrease in DTR would be expected as the LC/LU changed from predominantly rural to urban (urbanization).

The average DTR from station observations is larger during warm months (April–October) than during cold months (November–March). Since most stations are located in the eastern U.S., DTR from satellite measurements as averaged over the rural and urban stations follows the seasonal variations over the eastern U.S. and is larger in the spring and fall than in winter and summer. The diurnal range of  $T_s$  from satellite measurements is larger than that of  $T_a$  from station observations.

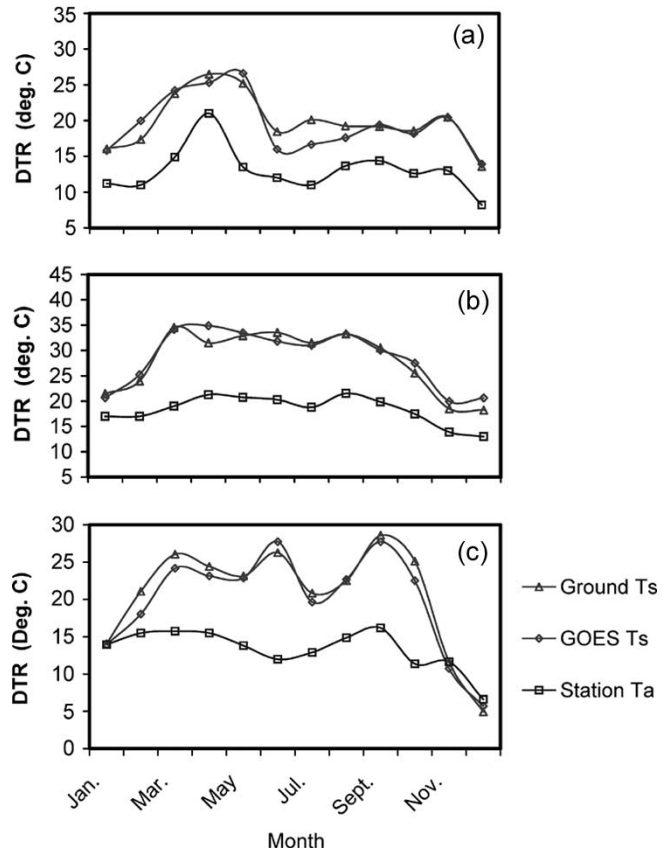


Fig. 5. Comparison of DTR of  $T_a$  from station observations and diurnal range of  $T_s$  from ground measurements and satellite retrievals under clear conditions at (a) Penn State, PA, (b) Boulder, CO, and (c) Ardmore, OK.

Satellite-based DTR is also larger in rural areas than in urban regions; the difference between rural and urban sites is smaller in summer and winter as compared to spring and fall.

In the above analysis, the diurnal range of air temperature from station observations is for all-sky conditions, while satellite-derived diurnal range of skin temperature is for clear conditions. In order to assess the effect of such differences, a comparison under the same conditions (all-sky or clear-sky) was conducted for two SURFRAD sites (Boulder, CO, 40.13° N, -105.24° W; and Penn State, PA, 40.72° N, 77.93° W), and one Oklahoma MESONET site (Ardmore, OK, 34.20° N, -97.15° W). Under all-sky conditions, the DTRs of  $T_s$ , as well as those of  $T_a$ , are largest in summer (July) at the eastern (Penn State, PA) and western (Boulder, CO) U.S. locations (Fig. 4). The diurnal range of  $T_s$  is larger than that of  $T_a$ , and they may not follow the same seasonal variations. The possible reason may be related to the effects of cloud radiative forcing (CRF), which depends on many factors, such as surface type or surface albedo, aerosol loading, water-vapor amount, cloud type, and cloud height [27], which may not be the same for  $T_s$  and  $T_a$ . Since the atmosphere near the surface reacts much more slowly to the effects of solar radiation than the surface [28], the phase of the diurnal range of  $T_a$  usually lags that of  $T_s$ .

Fig. 5 shows DTRs at three sites under clear conditions for  $T_a$  from station observations  $T_s$ , from ground measurements, and from GOES-8 estimates. Under clear conditions, the DTRs for  $T_a$ , as well as those for  $T_s$ , show similar seasonal variations,

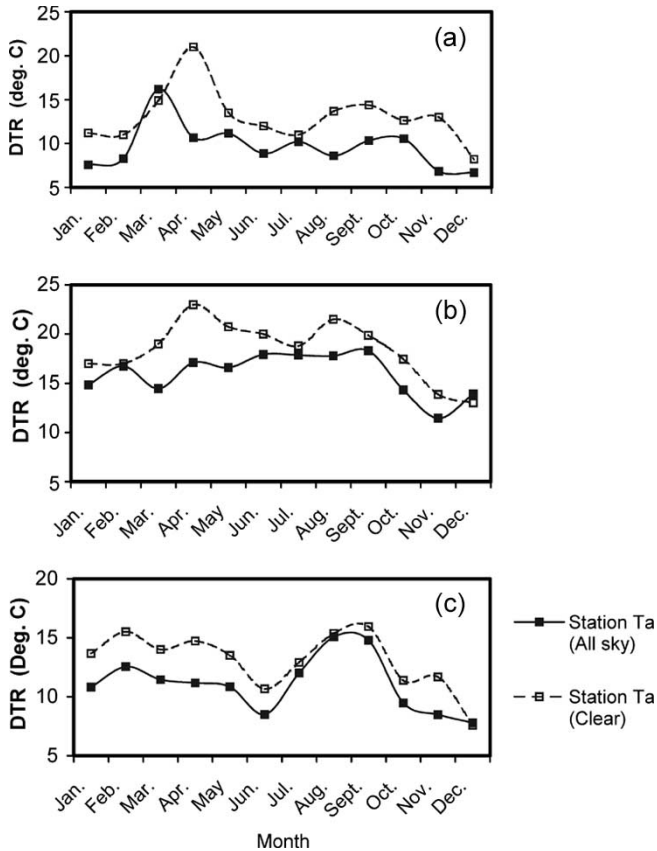


Fig. 6. Comparison of DTR of  $T_a$  from station observations under clear and all-sky conditions at (a) Penn State, PA, (b) Boulder, CO, and (c) Ardmore, OK.

as shown in Fig. 1, smaller in summer than for the other seasons over the eastern U.S. (Penn State, PA), while in the western part (Boulder, CO), largest in spring (May), followed by summer and fall, and smallest in winter. The diurnal range of  $T_a$  under clear-sky conditions is also observed to be smaller than that of  $T_s$ . Overall, the DTR derived from the GOES-8 measurements is close to that from the ground observations under clear-sky conditions.

Solar radiation can heat the surface much more rapidly than the air near the surface, resulting in larger  $T_s$  than  $T_a$  during daytime [28]; during nighttime, the surface emits longwave radiation and releases energy to the atmosphere, reducing  $T_s$  below  $T_a$ . Therefore, the DTR for  $T_s$  under both all-sky and clear-sky conditions is usually larger than that for  $T_a$ , as reported here.

#### D. Cloud Effects on DTR

In the above analysis, skin temperatures are stratified according to cloudiness. Clear conditions are considered if the daily average CCF is less than 10%, and a monthly mean is derived. DTRs for both  $T_a$  (Fig. 6) and  $T_s$  (Fig. 7) under clear conditions are usually larger than those under all-sky conditions. This is because the CRF has a cooling effect at the Earth’s surface during daytime [26] and suppresses the maximum temperature; during nighttime, clouds emit outgoing longwave radiation back to the surface, having a warming effect

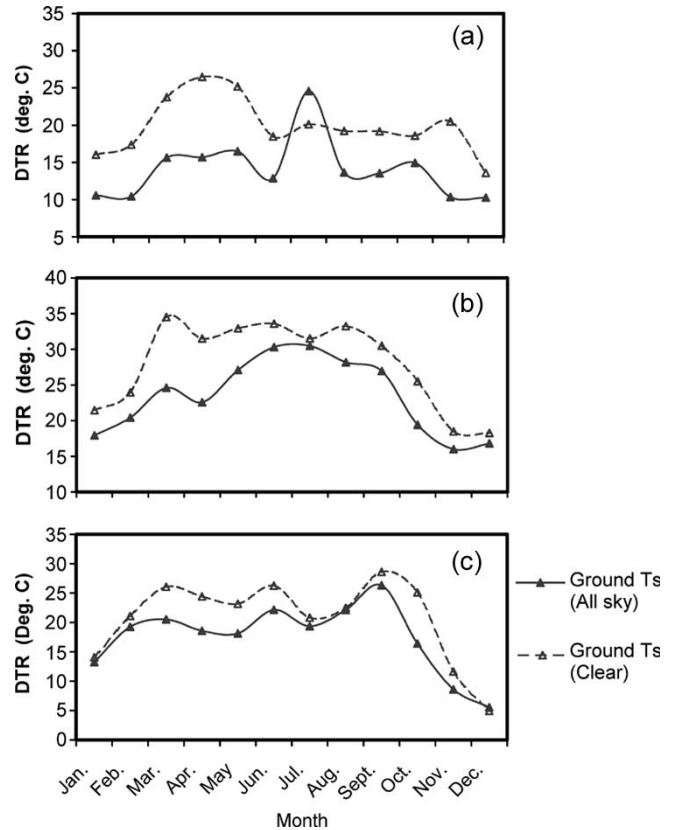


Fig. 7. Comparison of DTR of  $T_s$  from ground measurements under all-sky and clear-sky conditions at (a) Penn State, PA, (b) Boulder, CO, and (c) Ardmore, OK.

on the nighttime surface temperature, with strongest warming effect in winter [29]. The total effect of clouds is a decrease in DTR.

It is observed that during summer months, such as July–August, the differences in DTRs between clear- and all-sky conditions are smaller than during spring and fall, as shown in Figs. 6 and 7. This may be due to the effects of water-vapor radiative forcing (WRF). The water-vapor amount during warm months (May–September) is larger than during cold months (Fig. 6); it is usually larger under all-sky conditions than under clear-sky conditions. While during summer months, especially from July to August, a difference in water-vapor amount between all-sky and clear-sky conditions still exists over the western U.S. (Boulder, CO) [Fig. 8(b)], it is very small over the eastern (Penn State, PA) and middle south U.S. (Ardmore, OK) [Fig. 8(a) and (c)]. For the same amount of water vapor, the shortwave cooling effect of WRF is much greater for clear conditions than for all-sky conditions [26]. This situation is similar to the damping effect of clouds on DTR under all-sky conditions and, therefore, makes the difference in DTR between the clear- and all-sky conditions small. At the eastern U.S. (e.g., Penn State, PA) during summer (July), the DTR under the clear-sky can be even lower than that under all-sky conditions, which causes a dip of DTR in summer (Fig. 7). As shown in Fig. 9, water-vapor amount is higher over the eastern U.S. than in the western part; it is highest over the southeastern part during summer. The effect of WRF may be

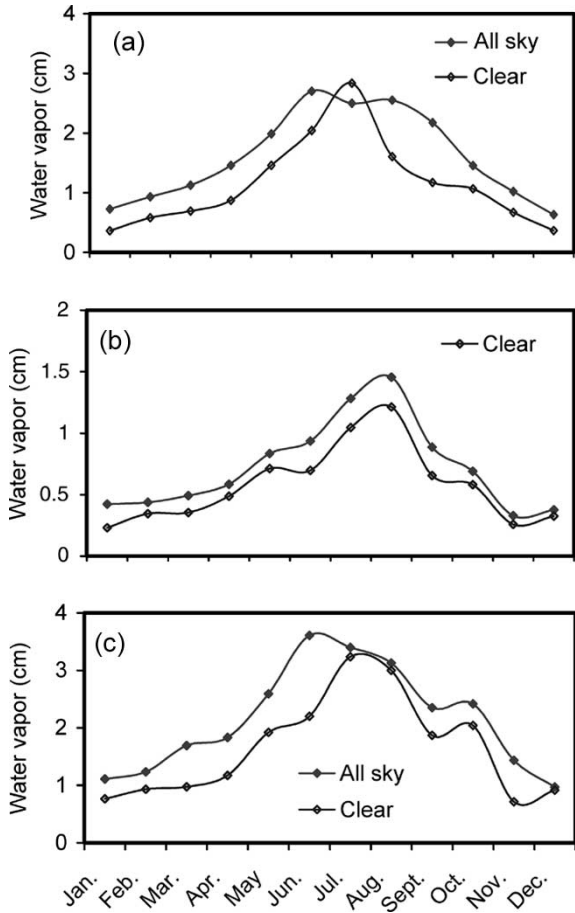


Fig. 8. Monthly mean atmospheric water vapor from the ETA model. (a) Penn State, PA. (b) Boulder, CO. (c) Ardmore, OK.

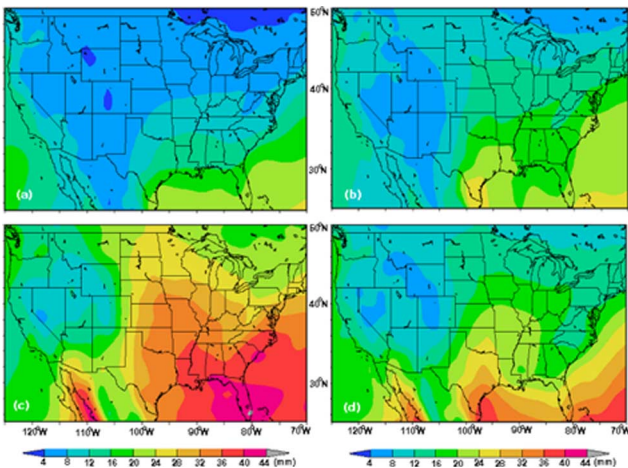


Fig. 9. Spatial distribution of water-vapor amount during (a) winter, (b) spring, (c) summer, and (d) fall as available from the ETA model.

another important factor for the decrease in DTR in summer under clear conditions over the southeastern U.S. [Fig. 1(c)].

IV. SUMMARY AND CONCLUSION

In this study, the feasibility to evaluate DTR from satellite observations that depict the diurnal cycle was investigated.

Since satellites have evenly distributed spatial coverage, they offer an advantage over sparse station observations of DTR. Specifically, proposed algorithms were applied to GOES-8 infrared measurements to derive surface skin temperature  $T_s$  and compute DTRs. These were compared to similar quantities based on station air temperatures  $T_a$  and ground observations of  $T_s$ , for several dominant LU categories and locations. Since the satellite DTRs are obtained under clear-sky conditions only, the effect of clouds on this parameter was assessed by subsetting the station observations into clear-sky conditions, and conducting independent comparisons for both clear and all-sky conditions. The five-year record of observations was stratified by seasons. A good agreement was found between the satellite estimates and those based on ground observations of  $T_s$ . When evaluated against ground observations from the SURFRAD and MESONET network, the accuracy in the satellite-derived DTRs is better than 1 °C, and the rms error is about 2 °C.

During all seasons, the satellite-based DTRs are larger over the midwest U.S. as compared to the eastern part and the northwest coast, which are more vegetated. In the western U.S., DTR is larger in warm seasons (spring, summer, and fall) than in cold seasons (winter), while over the eastern part, DTR is larger in spring and fall than in summer and winter. The station-observed DTR from  $T_a$  under all-sky conditions is larger in warm months (April–October) than in cold months (November–March), while the satellite-measured DTR for  $T_s$  under clear-sky conditions, as averaged over the weather stations, follows the seasonal variation in the eastern U.S. and is smaller in summer than in other seasons. For both station observations and satellite measurements, DTRs at rural stations usually have larger values than at urban stations.

The DTR of  $T_a$  is much smaller than that of  $T_s$  under both all-sky and clear-sky conditions and the phase lags that of  $T_s$ . Under all-sky conditions, the DTRs from ground measurements of  $T_s$  follow similar seasonal variations as those from station-observed  $T_a$ , and are larger in summer than in winter. While under clear-sky conditions, the DTRs for  $T_a$  from station observations follow similar seasonal variations as those for  $T_s$ . Clouds reduce DTRs for both skin and air temperatures. The effect of evapotranspiration from land vegetation and WRF contributes to the decrease of DTR in summer under clear conditions over the southeastern U.S.

It was demonstrated that geostationary satellites could be used for estimating DTRs at an accuracy that makes them attractive for climate-change studies. Moreover, the fact that satellites observe the surface only under clear-sky conditions could have an added benefit since the surface signals, which respond directly to climate change, can be detected. With the upcoming plans for GOES-R and the recognition in the scientific community for the need to maintain credible calibrations of the various satellites so that climate records can be constructed, the prospects for utilizing the approach presented in this study for long-term investigations are promising. Moreover, the plans of the World Climate Research Program of the World Meteorological Organization to have the globe covered by advanced geostationary satellites in the near future will provide an opportunity for global-scale applications. The effects of factors, such as clouds, soil moisture, LC/LU change, land

vegetation, greenhouse gases, and aerosols on DTR have been recognized. In-depth studies on the quantitative relationship between these factors and satellite-derived DTRs are needed so that the impacts of LU change due to natural or anthropogenic forcing, such as urbanization, deforestation, and agriculture development on regional climate (DTR), change over different areas of the globe can be undertaken.

## REFERENCES

- [1] K. Braganza, D. J. Karoly, and J. M. Arblaster, "Diurnal temperature range as an index of global climate change during the twentieth century," *Geophys. Res. Lett.*, vol. 31, no. 13, L13217, 2004.
- [2] Intergovernmental Panel on Climate Change, *Climate Change 2001: The Scientific Basis*, J. T. Houghton, Y. Ding, D. J. Griggs, M. Noguer, P. J. van der Linden, X. Dai, K. Maskell, C. A. Johnson, Eds. Cambridge, U.K.: Cambridge Univ. Press, 2001.
- [3] K. P. Gallo, T. W. Owen, and D. R. Easterling, "Temperature trends of the U.S. historical climatology network based on satellite-designated land use/land cover," *J. Clim.*, vol. 12, no. 5, pp. 1344–1348, 1999.
- [4] E. Kalnay and M. Cai, "Impact of urbanization and land use on climate change," *Nature*, vol. 423, no. 6939, pp. 528–531, May 2003.
- [5] D. R. Easterling, T. C. Peterson, and T. R. Karl, "On the development and use of homogenized climate datasets," *J. Clim.*, vol. 9, no. 6, pp. 1429–1434, 1996.
- [6] K. E. Trenberth. (2003). *Comment on Impact of Urbanization and Land-Use Change on Climate*. [Online]. Available: [http://stephenschneider.stanford.edu/Publications/PDF\\_Papers/Trenberth\\_KalnayComment.pdf](http://stephenschneider.stanford.edu/Publications/PDF_Papers/Trenberth_KalnayComment.pdf)
- [7] D. Stone and A. Weaver, "Factors contributing to diurnal temperature range trends in twentieth and twenty-first century simulations of the CCCma coupled model," *Clim. Dyn.*, vol. 20, no. 5, pp. 435–445, 2003.
- [8] H. S. Park and M. Joh, "Climate change due to the gradual increase in atmospheric CO<sub>2</sub>: A climate system model sensitivity study," *Key Eng. Mater.*, vol. 277–279, pp. 595–600, 2005.
- [9] D. J. Karoly and K. Braganza, "Attribution of recent temperature changes in the Australian region," *J. Clim.*, vol. 18, no. 3, pp. 457–464, 2005.
- [10] R. Schnur and K. I. Hasselmann, "Optimal filtering for Bayesian detection and attribution of climate change," *Clim. Dyn.*, vol. 24, no. 1, pp. 45–55, 2005.
- [11] M. Zhao and A. J. Pitman, "The relative impact of regional scale land cover change and increasing CO<sub>2</sub> over China," *Adv. Atmos. Sci.*, vol. 22, no. 1, pp. 58–68, 2005.
- [12] K. P. Gallo, D. R. Easterling, and T. C. Peterson, "The influence of land use land cover on climatological values of the diurnal temperature range," *J. Clim.*, vol. 9, no. 11, pp. 2941–2944, 1996.
- [13] M. Jin, R. E. Dickinson, and D. Zhang, "The footprint of urban areas on global climate as characterized by MODIS," *J. Clim.*, vol. 18, no. 10, pp. 1551–1565, May 2005.
- [14] A. Dai, K. E. Trenberth, and T. R. Karl, "Effects of clouds, soil moisture, precipitation, and water vapor on diurnal temperature range," *J. Clim.*, vol. 12, no. 8, pp. 2451–2473, 1999.
- [15] W. B. Rossow and E. Duenas, "The International Satellite Cloud Climatology Project (ISCCP) web site: An online resource for research," *Bull. Amer. Meteorol. Soc.*, vol. 85, no. 2, pp. 167–172, 2004.
- [16] M. Jin and R. Dickinson, "New observational evidence for global warming from satellite," *Geophys. Res. Lett.*, vol. 29, no. 10, 1400, pp. 39-1–39-4, 2002.
- [17] D. L. Sun and R. T. Pinker, "Estimation of land surface temperature from a Geostationary Operational Environmental Satellite (GOES-8)," *J. Geophys. Res.*, vol. 108, no. D11, 4326, pp. ACL-1–ACL-15, 2003.
- [18] —, "Case study of soil moisture's effect on land surface temperature retrieval," *IEEE Geosci. Remote Sens. Lett.*, vol. 1, no. 2, pp. 127–130, Apr. 2004.
- [19] Z. M. Wan, Y. L. Zhang, Q. C. Zhang, and Z. L. Li, "Validation of the land-surface temperature products retrieved from Terra Moderate Resolution Imaging Spectroradiometer Data," *Remote Sens. Environ.*, vol. 83, no. 1/2, pp. 163–180, Nov. 2002.
- [20] R. T. Pinker *et al.*, "Surface radiation budgets in support of the GEWEX Continental Scale International Project (GCIP)," *J. Geophys. Res.*, vol. 108, 2003, in press.
- [21] D. W. Keith and J. G. Anderson, "Accurate spectrally resolved infrared radiance observation from space: Implications for the detection of decade-to-century-scale climatic change," *J. Clim.*, vol. 14, no. 5, pp. 979–990, 2001.
- [22] B. B. Hicks, J. J. DeLuisi, and D. R. Matt, "The NOAA Integrated Surface Irradiance Study (ISIS)—A new surface radiation monitoring program," *Bull. Amer. Meteorol. Soc.*, vol. 77, no. 12, pp. 2857–2864, 1996.
- [23] D. R. Easterling, T. C. Peterson, and T. R. Karl, "On the development and use of homogenized climate datasets," *J. Clim.*, vol. 9, no. 6, pp. 1429–1434, 1996.
- [24] C. J. Willmott, C. M. Rowe, and Y. Mintz, "Climatology of the terrestrial seasonal water cycle," *J. Clim.*, vol. 5, no. 6, pp. 589–606, Nov./Dec. 1985.
- [25] D. L. Sun, R. T. Pinker, and M. Kafatos, "The variations of satellite-derived diurnal temperature range over the United States," *Geophys. Res. Lett.*, vol. 33, no. L05705, 2006, to be published.
- [26] I. Durre and J. M. Wallace, "The warm season dip in diurnal temperature range over the eastern United States," *J. Clim.*, vol. 14, no. 3, pp. 354–360, 2001.
- [27] Z. Li and A. Trishchenko, "Quantifying the uncertainties in determining SW cloud radiative forcing and cloud absorption due to variability in atmospheric conditions," *J. Atmos. Sci.*, vol. 58, no. 4, pp. 376–389, Feb. 2001.
- [28] D. P. Duda and P. Minnis, "A study of skin temperature/cloud shadowing relationships at the ARM SGP site," presented at the 10th ARM Science Team Meeting, San Antonio, TX, Mar. 13–17, 2000.
- [29] S. K. Gupta, W. F. Staylor, W. L. Darnell, A. C. Wilber, and N. A. Richey, "Seasonal-variation of surface and atmospheric cloud radiative forcing over the globe derived from the satellite data," *Geophys. Res. Lett.*, vol. 98, no. D11, pp. 20761–20778, 1993.



**Donglian Sun** received the Ph.D. degree from the University of Maryland, College Park, in 2003.

She is currently a Research Scientist at the Center for Earth Observing and Space Research at George Mason University. Her research interests focus on information retrieval from remotely sensed data, numerical model simulations of tropical storms, and remote-sensing applications to coastal problems.



**Menas Kafatos** received the Ph.D. degree in physics from the Massachusetts Institute of Technology, Cambridge, in 1972.

He is currently with George Mason University, Fairfax, VA, where he is a Dean, a University Professor of interdisciplinary science, the Director of the Center for Earth Observing and Space Research, and the Founding Dean of the College of Science. His main research interest is earth system science including remote sensing applications in natural hazards such as hurricanes, and vegetation and climate studies.



**Rachel T. Pinker** received the Ph.D. degree from the University of Maryland, College Park, in 1976.

She is currently a Professor in the Department of Atmospheric and Oceanic Science, University of Maryland. Her research interests are in the area of remote sensing and surface-atmosphere interactions.



**David R. Easterling** received the Ph.D. degree from the Department of Geography, University of North Carolina, Chapel Hill, in 1987.

He is currently the Chief of the Scientific Services Division, National Climatic Data Center, National Oceanic and Atmospheric Administration, Asheville, NC. He is also a contributor to the Intergovernmental Panel on Climate Change Assessment Reports. His research interests include the detection of climate change in the observed record, particularly changes in extreme climate events.